A DEMONSTRATION 1D WAVEGUIDE FOR THE INTELLIGENT DISTRIBUTED ACOUSTIC SENSOR (IDAS

Daniel Finfer	Silixa Ltd, 230 Centennial Drive, Elstree HERTS, WD6 3SN
Veronique Mahue	Silixa Ltd, 230 Centennial Drive, Elstree HERTS, WD6 3SN
Andrew Clarke	Silixa Ltd, 230 Centennial Drive, Elstree HERTS, WD6 3SN
Douglas Miller	Department of Earth, Atmospheric and Planetary Sciences, Massachusetts Institute of Technology, Cambridge MA USA 02139
Tom Parker	Silixa Ltd, 230 Centennial Drive, Elstree HERTS, WD6 3SN
Mahmoud Farhadiroushan	Silixa Ltd, 230 Centennial Drive, Elstree HERTS, WD6 3SN

1 INTRODUCTION

Distributed acoustic sensor technology makes it possible to observe the acoustic field at every point along a length of optical fibre up to several kilometres in length. A demonstration rig was built to help illustrate Silixa's intelligent Distributed Acoustic Sensor (iDAS^{TM}) to collaborators. The iDAS tube wave demonstration rig is comprised of a PVS measuring 1.5 m in height which is filled with water and wrapped on its exterior with several tens of meters of fibre optic cable. The waveguide was excited acoustically by injecting air bubbles at the bottom of the tube using an air compressor. This paper describes how iDAS technology is used with array processing to track bubble-generated acoustic energy. This bubble-generated energy can be used to monitor changes in the void fraction within the waveguide.

2 THE IDAS WAVEGUIDE DEMONSTRATION RIG

The iDAS makes it possible to observe the acoustic signal at every point along a length of fibre optic cable. This is accomplished by firing a laser into fibre optic cable several times per second. By time-gating the backscatter and measuring its change in time, it is possible to determine the acoustic signal at every meter along a fibre optical cable several kilometers in length. Applications for this novel technology in seismic measurement, flow monitoring, acoustic field visualization, and security systems have been described elsewhere[1-3].

In order to demonstrate the capabilities of iDAS both in the laboratory and at exhibitions, a small system demonstration rig was built. The demonstration system uses iDAS to monitor bubbles emitted into a water-filled, vertically-mounted PVC pipe. This section describes the layout and basic functioning of the system.

2.1 Physical layout

The iDAS waveguide demonstration system consists of a vertically-mounted PVC tube which has been wrapped with unmodified fibre optic cable. The tube is partially filled with water, and has an injector at base which is fitted with a one-way valve to prevent leaks. A tube leads from to the injector inlet from a small pressure manifold. The manifold is used to control the pressure delivered to the air inlet, and features an unused inlet to allow additional compression to be added to the system for specialized testing. The principal dimensions of the demonstration are shown below in Figure 1.

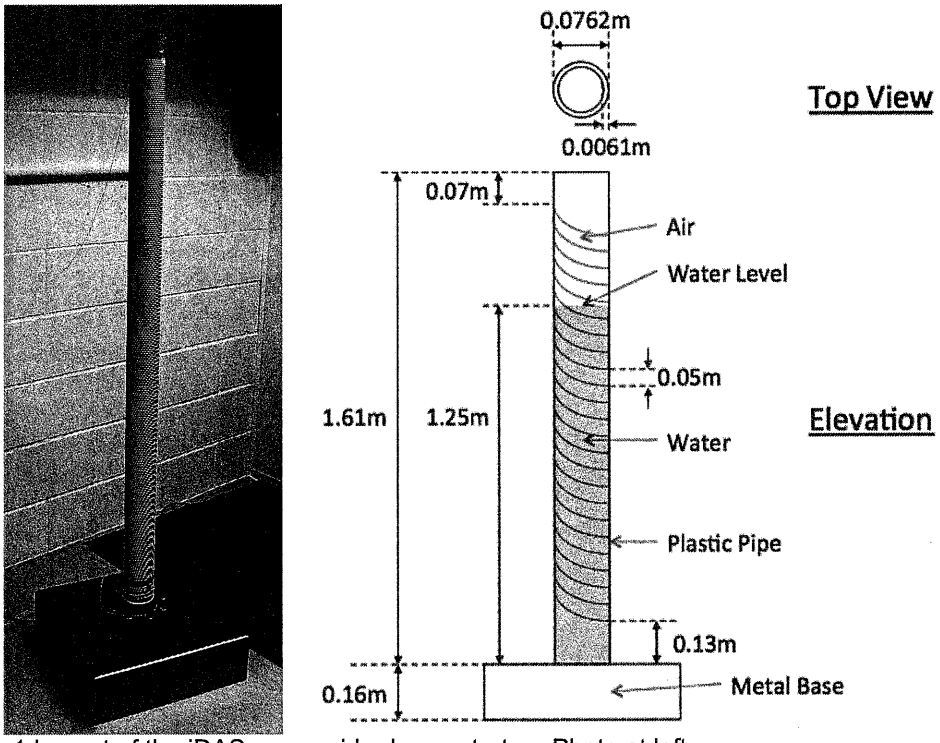

Figure 1 Layout of the iDAS waveguide demonstrator. Photo at left.

2.2 Single bubble emissions

Basic system functionality can be demonstrated by monitoring the signal generated as individual bubbles are injected into the water column. A sample of the acoustic signal observed by iDAS at a single point as individual bubbles are injected into the water is shown below in Figure 2. It is well-known that frequency emitted as bubbles injected into a water column can be used to size bubbles. Standard Fourier transform methods can be applied to the signal to show that principal oscillation here is around 600 Hz. For air bubbles in water with resonances much below several tens of kilohertz, the surface tensions effects are nearly negligible, and it is reasonable to use Minnaert's estimate for bubble resonance[4,5].

$$\omega_M = \frac{1}{R_0}\sqrt{\frac{3\gamma p_0}{\rho}} \qquad (2.1)$$

where ω_M is the Minnaert resonance frequency, R_0 is the bubble equilibrium radius, γ is the ratio of specific heats for air, p_0 is the equilibrium pressure, and ρ is the density of water. For the conditions of observation, the 600 Hz ringing corresponds to a bubble radius of around 5 mm.

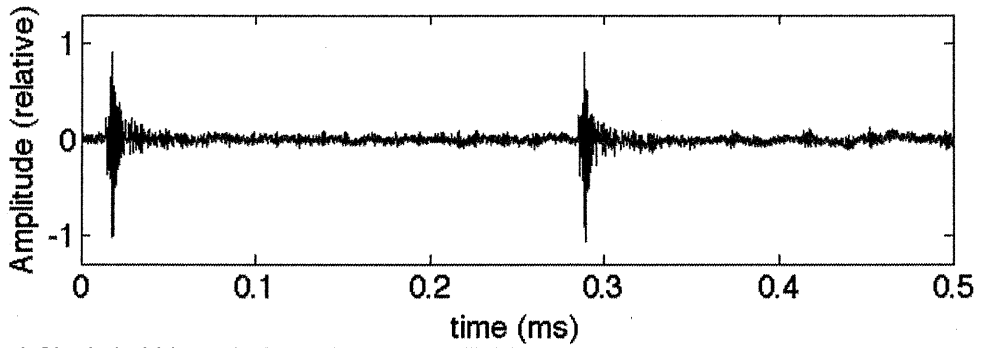

Figure 2 Single bubble emissions observed on iDAS.

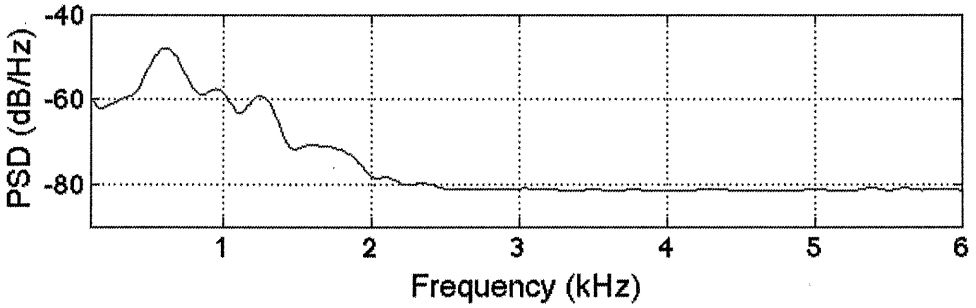

Figure 3 Frequency spectrum for bubbles shown in Figure 2. Averaged over 20 bubble emissions.

Thus, iDAS can be used for sizing bubbles based on passive emissions, and so can be used to quantify the amount of gas emitted by subsea gas leaks both in the lab and in the field[6] using already-established methods[7]. In order to characterize smaller bubbles properly, field applications for gas leak quantification are dependent on the broadband sensitivity for the iDAS system which has already been demonstrated[1].

3 THE IDAS WAVEGUIDE DEMONSTRATION TEST

Since the iDAS system is capable of simultaneously monitoring the signal in discrete sections along the entire length of a fibre optic cable, this system effectively renders any fibre optic cable into a multi-element array receiver. In the case of the iDAS waveguide demonstration rig, it was desired to illustrate the way in which distributed fibre optic sensing can be used with array processing to monitor the wavespeed within a waveguide. In this section, the experiment shown in the previous section above is repeated, but the acoustic results as recorded along the entire pipe are shown. Then, that result is processed to show the wavespeed for the system. Finally, the gas hold-up of the mixture is increased, and the change in sound speed is used to indicate a change in the void fraction.

3.1 Wavespeed measurement in a 1D waveguide

The acoustic field resulting from the emission of a single bubble by the bubble injector is shown in Figure 4. In this figure, the bubble is emitted at t=0ms. It is seen that the signal radiated by the bubble at the bottom of the tube propagates upward, and is reflected at the pressure release surface encountered at the sea-air interface. A phase-inverted version of the signal travels downwards, and further reverberation is then visible.

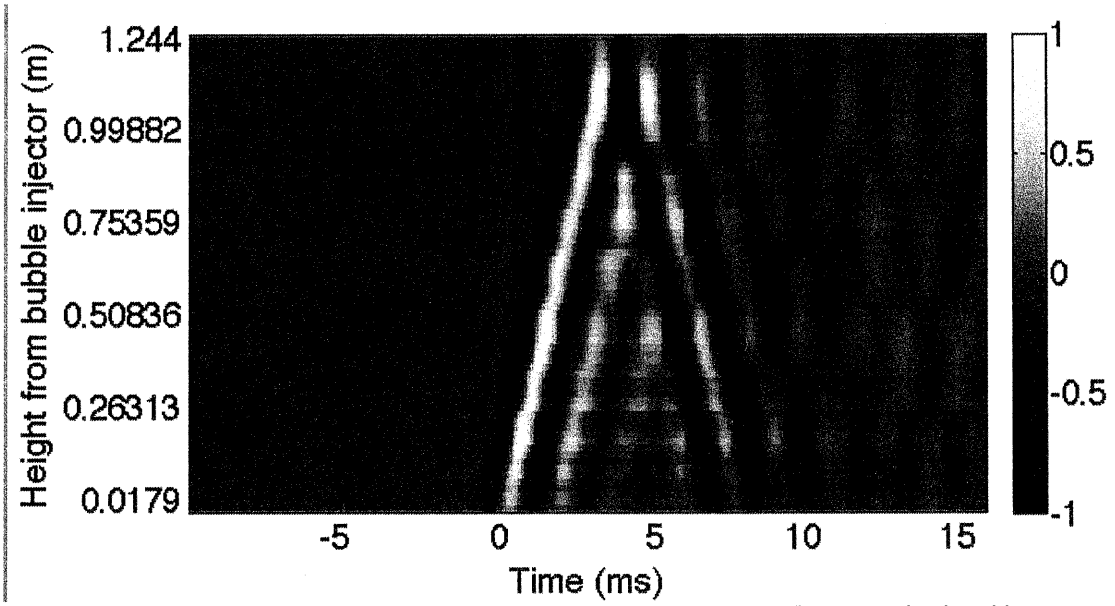

Figure 4 Single bubble emission as seen over the entire iDAS array. The acoustic signal is displayed in normalised amplitude.

Signals of the type shown in Figure 4 can be examined using kω plots, from which the velocity of propagation can be determined accurately[2]. The kω plot for the case where single bubbles having radius 5 mm and are emitted at intervals of approximately 0.3 sec is shown below in Figure 5.

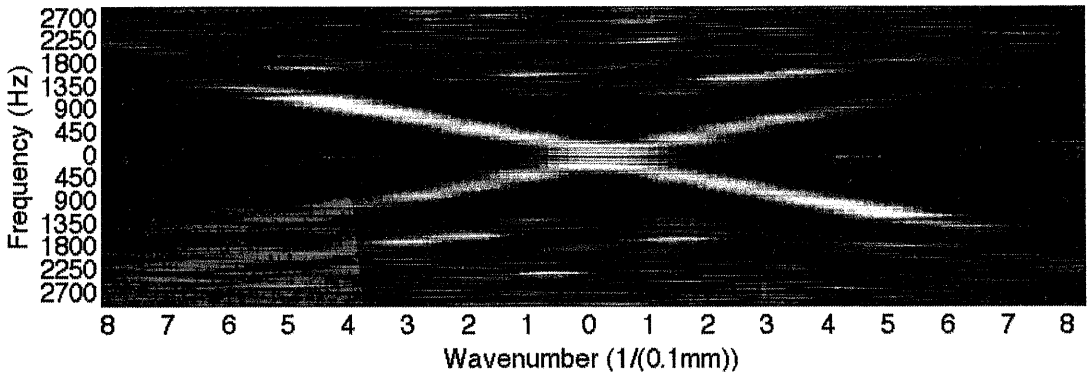

Figure 5 Low void fraction kω observed over the entire iDAS array. Acoustic signal is displayed in normalised amplitude.

By analysing the slope of lines which appear within the kω domain and which pass through the orgin, the corresponding velocities of propgation for that environment can be determined. A scan of the angles represented by the 'x' shape visible within Figure 5 reveals that the primary wavespeed within the waveguide is approximately 363 m s^{-1}. This speed is lower than the speed of sound for fresh water in an infinite medium[8], which at STP is approximately 1497 m s^{-1}. This deviation can be explained as a result of two effects: wall compliance and bubble entrainment. The compliance of the tube walls can be analysed using the approach of Wylie and Streeter[9], from which the speed of sound can be shown to be as formulated below.

$$c_{tube} = \sqrt{\frac{1}{\rho\left(K_\Gamma + \frac{d\left(1-\frac{\mu}{2}\right)}{e\ Y}\right)}} \qquad (3.1)$$

The sound speed within a tube c_{tube} has been expressed above where d is diameter, K_f is the isothermal compressibility, e is wall-thickness, Y is the Young's modulus for the pipe, and μ is the dynamic viscosity of the water. Here, the quantity $(1-\mu/2)$ is a 'structural coefficient' which has been introduced to account for the fact that the pipe is thin-walled and fixed only at one end. Substituting the values for this environment (ρ=1500 kg m^{-3}; K_f =0.435 x 10^{-9} Pa^{-1}; d = 88.9 mm; e=6.35 mm; μ = 1 Pa s; and Y = 2.8 GPa), an estimated sound speed of 460 m s^{-1} is obtained. The sound speed of 363 m s^{-1} which is seen in the experimental results has been further reduced by the presence of gas within the water, as can be accounted for using a standard approach[4].

3.2 Void fraction measurement in a 1D waveguide

Once the sound speed for pure water in this environment has been predicted (via Wylie and Streeter), it is possible to observe the effect of increased void fraction on sound within the pipe. It is well-known that an increased number of disperse bubbles having radii far above the excitation frequency should lead to a reduction in the propagation speed of the bulk medium. That effect is observed here.

For this test, a high capacity air compressor was introduced onto the system, and the bubble injection rate was increased. This increase in bubble injection rate resulted in both a higher void fraction, and the circulation of microbubbles which reduced the stiffness of the bulk fluid and hence the entire system. The results of this test are shown below.

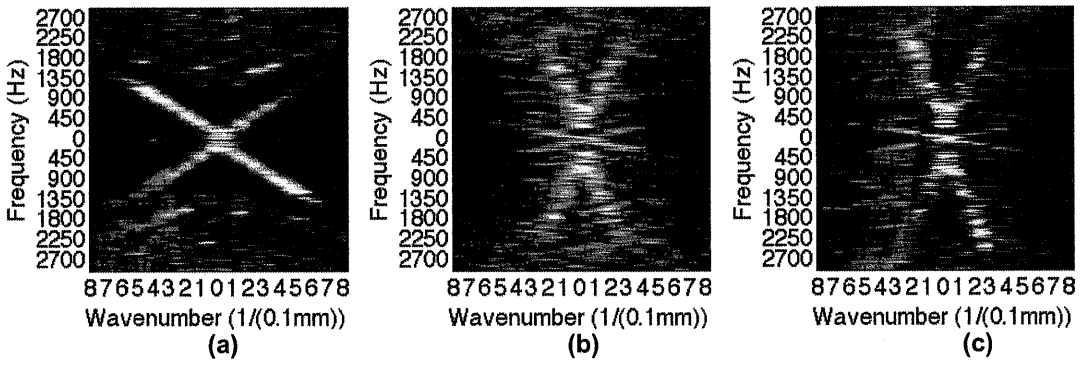

Figure 6 Effect of varying the void fraction on the sound speeds observed within the pipe. **(a)** Low void fraction; principle speed of 363 m s^{-1} is visible. **(b)** Higher void fraction. Two speeds are visible: (1) 120 m s^{-1}, which corresponds to the low speed of the bubbly bulk fluid, and (2) 1600 m s^{-1}, which corresponds to a now-undamped structural mode supported by the PVC pipe walls. **(c)** Higher void fraction after 10 minutes of sustained bubble circulation leads to a slightly lower speed for the bulk fluid medium of 98 m s^{-1}. The weakly damped structural mode continues to be visible.

The results for the test wherein void fraction was varied are shown in Figure 6. Figure 6 (a) shows the same result as Figure 5. Visible here is the speed of 363 m s^{-1}, and the signal bandwidth which extends out to around 1400 Hz. Immediately after the compressor was changed and higher bubble levels were introduced, a second measurement was taken, the results of which are shown in Figure 6 (b). Several interesting features stand out when comparing figure (a) to figure (b). In figure (b), the sound speed corresponding to the propagation through the bulk fluid has reduced to around 120 m s^{-2}. This drop in sound speed is a result of the increased void fraction. Secondly, the maximum detectable frequency of propagating signal within the fluid has dropped to around 600 Hz. This reduction in bandwidth is a result of attenuation caused by the gas bubbles in the liquid. Third, an additional sound speed of around 1600 m s^{-1} has become visible in figure (b). This is a structural wave which, in the absence of bubbles, was suppressed by the stiffness of the fluid within the pipe. However, once the void fraction within the fluid was increased, the stiffness of the bulk fluid was reduced and the structural wave encountered a lower impedance. Figure 6 (c) was produced after the high void fraction circulation had been in steady state for several minutes. The increased gas

content within the fluid here led to an even lower sound speed for the bulk fluid medium (around 98 m s^{-1}), and the structural wave first observed in figure (b) remained visible.

4 CONCLUSIONS

A compact demonstration wavetube was developed to display the ability for iDAS to monitor both single bubble emissions, and track wave propagation within a waveguide. Analysis of data gathered using iDAS in this configuration indicated novel ability to monitor acoustic propagation within waveguides. The demonstration wavetube showed how it might be possible to use iDAS for instance to quantify gas leaks in a subsea environment. Further, it was shown that array processing methods can be applied to map small changes in the acoustic propagation. These array methods make it possible to see clearly where multiple sound speeds are simultaneously supported by a given waveguide, and observe any changes of those sounds speeds over time.

5 ACKNOWLEDGEMENTS

The authors gratefully acknowledge the contributions of Ze Chen and Lovynash Dokhee in the development of this demonstration system. Kind thanks are also extended to Svetlin Staykov for his help with high pressure bubble generation.

6 REFERENCES

1. T. Parker, S.V. Shatalin., M. Farhadiroushan, Y. I. Kamil, A. Gillies, D. Finfer, and G. Efstathopoulos. 'Distributed Acoustic Sensing - A New Tool for Seismic Applications', 74th EAGE Conference & Exhibition incorporating SPE EUROPEC 2012, Y002 (June 2012).
2. K. Johannessen, B. Drakeley, M. Farhadiroushan, 'Distributed Acoustic Sensing – a new way of listening to your well/reservoir', SPE 149602 (2012).
3. G. Efstathopoulos, D. Finfer, Y. Kamil, S. Shatalin, T. Parker, and M. Farhadiroushan, 'Tracking system developed using an optical fiber-based distributed acoustic sensor', J. Acoust. Soc. Am. 130(4) 2450-2450 (2011).
4. T. G. Leighton, *The Acoustic Bubble*. London: Academic Press (1994).
5. M. Minnaert, 'On musical air-bubbles and sounds of running water', *Philisophical Magazine,* vol. 16, pp. 235-248 (1933).
6. A. Chalari, M. Mondanos, D. Finfer, D. Christodoulou, S. Kordella, G. Papatheodorou, M. Geraga, G. Ferentinos, 'Short-term monitoring of a gas seep field in the Katakolo bay (Western Greece) using Raman spectra DTS and DAS fibre-optic methods', Amer. Geophys. Union, (December 2012)
7. T.G. Leighton and P.R. White, 'Quantification of undersea gas leaks from carbon capture and storage facilities, from pipelines and from methane seeps, by their acoustic emssions', Proc. Roy. Soc. A, 468, 485-410 (2012).
8. J. Lubbers and R. Graaff, 'A simple and accurate formula for the sound velocity in water', Ultrasound Med. Biol. 24(7), 1065 (1998).
9. E.B Wylie and V.L. Streeter, *Fluid Transients in Systems,* Prentice-Hall (1993).